Some properties of the mixed $GaS_{0.4}Se_{0.6}$ nonlinear crystal in comparison to GaSe

Georgi Marchev[a)], Aleksey Tyazhev[a)], Vladimir Panyutin[a)], Valentin Petrov[a], Frank Noack,[a)]
Kentaro Miyata[a)], Michael Griepentrog[b)]

[a]Max-Born-Institute for Nonlinear Optics and Ultrafast Spectroscopy,
2A Max-Born-Str., D-12489 Berlin, Germany;
[b]Federal Institute for Materials Research and Testing (BAM), Division VI.4 Surface Technology,
87 Unter den Eichen, D-12205 Berlin, Germany

ABSTRACT

Two essential advantages can be expected from adding S to the well known nonlinear crystal GaSe: increase of the band-gap value or the short wave cut-off limit and improved hardness. Recently, we confirmed that the non-centrosymmetric structure of GaSe is preserved up to a GaS content of 40 mol. % while the nonlinear coefficient d_{22} is reduced by only 24%. The increased band-gap results also in higher surface damage threshold. Our preliminary Sellmeier equations for $GaS_{0.4}Se_{0.6}$ were based on refractive index measurements. These equations are refined in the present work by fitting second-harmonic generation and optical parametric amplification phase-matching angle data in the mid-infrared as well as birefringence data in the visible and near-infrared obtained with thin phase retardation plates. The two-photon absorption effect was studied for $GaS_{0.4}Se_{0.6}$ and GaSe using amplified picosecond pulses at 1064 nm, at a repetition rate of 10 Hz. For intensities in the GW/cm^2 range, the two-photon absorption coefficient of $GaS_{0.4}Se_{0.6}$ for the o-polarization is 3.5 times smaller than the corresponding coefficient of GaSe. This means that $GaS_{0.4}Se_{0.6}$ could be safely used in Nd:YAG laser pumped nanosecond optical parametric oscillators or picosecond optical parametric amplifiers, without nonlinear absorption losses. The dynamic indentation measurements with Berkovich type indenter of *c*-cut $GaS_{0.4}Se_{0.6}$ and GaSe plates indicate about 30% higher indentation modulus and microhardness of $GaS_{0.4}Se_{0.6}$ in comparison to GaSe.

Key words: nonlinear optical crystals; birefringence; two-photon absorption; microhardness; mid-infrared.

1. INTRODUCTION

Nonlinear crystals with composition GaS_xSe_{1-x}, x=0.2 and 0.4, were studied as early as 1982.[1] Relative measurements of the second-harmonic generation (SHG) conversion efficiency with a Q-switched CO_2 laser, yielding d_{22}(x=0.2)= (0.525±0.05)d_{22}(GaSe) and d_{22}(x=0.4)=(0.31±0.05)d_{22}(GaSe), indicated substantial reduction of the nonlinear coefficient with the S content. This together with the observed deterioration of the crystal quality in comparison to the two parent compounds, GaS and GaSe, obviously contributed to the lacking interest in further investigation of such solid solutions.

According to Ref. 1, a phase transition from the non-centrosymmetric (ε) phase of GaSe, corresponding to the $\bar{6}m2$ point group, to a centrosymmetric (β) phase, corresponding to the 6/*mmm* point group, takes place for 0.2<x<0.3. In Ref. 2, the limits of the possible polytypes occurring in the GaS_xSe_{1-x} solid solutions were given as: ε for x=0 (GaSe) to x~0.01, ε – γ mixture for x between ~0.01 and ~0.03, γ for x between ~0.05 and ~0.4, and β for x from ~0.5 to 1 (GaS). Here, the γ phase corresponds to the non-centrosymmetric point group 3m. More recent studies associated the mixed ε–γ phase with 0≤x≤0.4, a mixture of ε–γ and β was observed for x=0.5 and pure β phase for GaS,[3] see Ref. 4 for an overview. Nevertheless, the question about the transitions between the phases is very complex and has not found a satisfactory solution, yet. Four phases were identified for GaSe itself in the literature while GaS crystallizes only in the

Nonlinear Frequency Generation and Conversion: Materials, Devices, and Applications X,
edited by Konstantin L. Vodopyanov, Proc. of SPIE Vol. 7917, 79171G · © 2011 SPIE
CCC code: 0277-786X/11/$18 · doi: 10.1117/12.874452

β–phase. The literature on GaS_xSe_{1-x} compounds is often controversial concerning this issue and it seems that there is some dependence on the growth conditions.[5,6]

The first phase-matched nonlinear process realized with GaS_xSe_{1-x} crystals was difference-frequency generation from 7 to 12.5 μm with $GaS_{0.2}Se_{0.8}$.[1] More recently the phase-matching properties of a series of solid solutions with x ranging from 0.04 to 0.412 were measured for SHG of 2.79 μm (Er:YSGG laser) and 9.56/9.58 μm (CO_2 laser) radiation.[7,8] These authors speculated that the conversion efficiency with $GaS_{0.09}Se_{0.91}$ is 2.4 times higher than that of pure GaSe,[8] and approximately so much higher in comparison to In-doped GaSe.[7] However, this contradicts the general trend observed as a function of the band-gap, which grows with S-content but decreases with In-content,[9] as well as the conclusions in Ref. 1. Indeed our own measurements by SHG with femtosecond pulses at 4.65 μm gave d_{22}(x=0.05)=0.89 d_{22}(GaSe), d_{22}(x=0.1)=0.86 d_{22}(GaSe), and d_{22}(x=0.4)=0.76 d_{22}(GaSe).[10] This result, together with the large band-gap of $GaS_{0.4}Se_{0.6}$ (the composition close to the maximum S-content in the non-centrosymmetric structure), means that such nonlinear crystals are good candidates for application in 1064 nm pumped optical parametric oscillators (OPOs), generators (OPGs), and amplifiers (OPAs).

Two essential advantages can be expected from adding S to the well known nonlinear crystal GaSe: increase of the band-gap value or the short wave cut-off limit[11,12] and increased hardness[13] which is one of the basic limitations of GaSe. In our recent work[10] we estimated a band-gap of 2.278 eV (545 nm) for $GaS_{0.4}Se_{0.6}$ and a useful transparency range at the 3 cm^{-1} absorption level of 0.57-14.2 μm. These parameters are 1.972 eV (629 nm) and 0.64 to 18 μm, respectively, for GaSe. In accordance with the larger band-gap, the damage threshold for $GaS_{0.4}Se_{0.6}$, both for nanosecond pulses and continuous-wave radiation, was roughly 50% higher than for pure GaSe.[10] In addition, preliminary Sellmeier equations for $GaS_{0.4}Se_{0.6}$ were presented in Ref. 10 which were based only on refractive index measurements in the 0.633 – 10.0 μm spectral range. The present work reports (i) refinement of these dispersion relations based on phase-matched SHG data, (ii) estimation of the two-photon-absorption (TPA) coefficient at 1064 nm, relative to GaSe, and (iii) measurements of the microhardness of $GaS_{0.4}Se_{0.6}$ and GaSe under identical conditions.

2. CRYSTAL GROWTH

$GaS_{0.4}Se_{0.6}$ and GaSe crystals were grown using high purity Ga (99.9999%), Se (99.999%) and S (99.999%). The measured melting temperature was (960 ± 10)ºC. Single crystals were grown by the Bridgman-Stockbarger method in quartz ampoules with a diameter of 14 mm. The crystallization front velocity was 3 mm/day and the whole growth process took 20-25 days. Uniform single crystals up to 60 mm in length were grown, see Fig. 1.

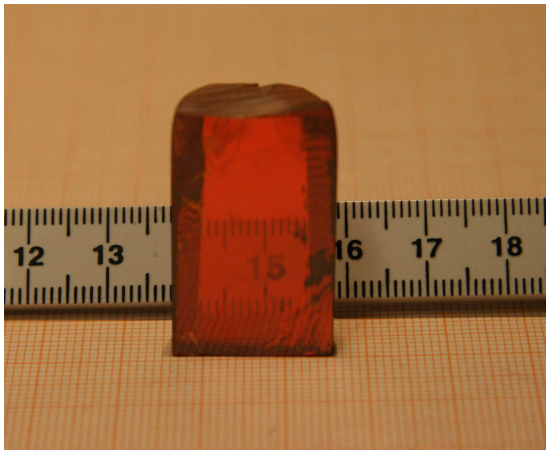

Fig. 1. Part of an as-grown $GaS_{0.4}Se_{0.6}$ boule showing the transparency of this composition.

The composition of the crystals grown was studied by electron microanalysis using INCA energy analytical system (Oxford Instruments) attached to a scanning electron microscope (JEOL JSM-5910LV). Plates of GaSe and $GaS_{0.4}Se_{0.6}$ were used for this purpose, which were cleaved from the central parts of the boules. Six points spread over an area of 1.5 cm^2 were tested for GaSe and eight points spread over an area of 2 cm^2 were tested in $GaS_{0.4}Se_{0.6}$. The average composition of GaSe was found to correspond to the chemical formula $Ga_{1.015}Se_{0.985}$. The composition with minimum Ga content corresponded to the stoichiometric one, GaSe, whereas the composition with maximum Ga content had a chemical formula of $Ga_{1.033}Se_{0.967}$. These results deviate substantially from the observations in Ref. 6 where a typical crystal composition of say $Ga_{0.92}Se_{1.08}$ corresponds to much larger and opposite in sign deviation from stoichiometry.

The average composition determined for x=0.4 was $Ga_{1.008}S_{0.407}Se_{0.585}$. The excess of Ga indicates the same direction of deviation from stoichiometry as in GaSe but this deviation is twice smaller. The Se and S deviations are in opposite directions leading to an average cation-anion deviation of 0.8 at. %. The composition with minimum Ga content corresponds to the one with maximum S content and the chemical formula $Ga_{0.978}S_{0.438}Se_{0.584}$ whereas the composition with maximum Ga content corresponds to the one with minimum Se content and the chemical formula $Ga_{1.021}S_{0.404}Se_{0.575}$. The composition with minimum S content is $Ga_{1.010}S_{0.391}Se_{0.599}$, the same for which the Se content is maximized.

3. DISPERSION AND BIREFRINGENCE

The Sellmeier fits for $GaS_{0.4}Se_{0.6}$ were refined based on experimental data from measurements with phase retardation plates which were 0.26 and 0.87 mm thick, at three wavelengths, λ = 0.6328, 1.0642 and 1.9425 μm, and phase-matched SHG as well as OPA processes.

$GaS_{0.4}Se_{0.6}$, similarly to GaSe, exhibits large birefringence (>0.3). Since both crystals are easily cleaved in planes perpendicular to the optic axis, this can be used to realize phase retardation plates. For instance, using such *c*-cut plates with a thickness ~1 mm and varying the angle of incidence between 0 and 10-15°, it is possible to continuously vary the phase retardation from 0 to few radians and change the polarization state of the transmitted beam.

In such an experiment a $GaS_{0.4}Se_{0.6}$ plate was positioned between two crossed polarizers and rotated about an axis, normal to the incidence plane defined by the wave vector *k* and the crystal axis *c*. This results in different transmission through the second polarizer (analyzer) in dependence on the angle of rotation α. The polarization of the incident radiation, defined by the first polarizer, was at an angle 45° with respect to the axis of rotation. The transmission is defined by $T = \sin^2(\phi)$, where $\phi = \pi \Delta n(\gamma) L/(\lambda \cos\gamma)$, $\Delta n(\gamma) = n_o - n_e(\gamma)$, L - plate thickness, and the angle γ is defined from $\sin(\gamma) = \sin(\alpha)/n_o$. The angle α was measured for values corresponding to minimum transmission. The k-th minimum in the transmission dependence (k = 0 refers to $k//c$), obtained at $\phi = k\pi$, corresponds to the relation $\Delta n = n_o (1 - 1/\varepsilon)$, where $\varepsilon^2 = 1 + n_o^2 (\delta^2 - 1)/\sin^2\alpha$, $\delta = 1 - Rb/n_o$, $R = k\lambda/L$, and $b^2 = 1 - (n_o)^{-2}\sin^2\alpha$. Experimentally, we measured k = 1, 2, and 3 orders. The measured dependence of Δn on n_o appears to be linear in the given interval $[n_o]$ which was selected from our measurements of the index of refraction by the minimum deviation method with a semiprism.[10] This dependence is presented in Table 1 in the parametric form $\Delta n = bn_o - a$.

Table 1. Birefringence Δn of $GaS_{0.4}Se_{0.6}$ measured at three wavelengths λ with the help of phase-retardation plates and crossed polarizers.

λ [μm]	*a*	*b*	$[n_o]$	n_o	Δn
0.6328	0.2658	0.2081	[2.77 - 2.81]	2.7880	0.3144
1.0642	0.2658	0.2165	[2.66 - 2.70]	2.6788	0.3142
1.9425	0.2638	0.2175	[2.62 - 2.66]	2.6400	0.3104

For refinement of the index of refraction in the mid-IR we used critical angle data from phase-matched SHG (oo-e type-I) and OPA (eo-e type-II) experiments. This data is included in Table 2 in terms of external (experimental) incidence angles. In Ref. 8 such angles of incidence were given for the compositions x = 0.369 and x = 0.412 and we reduced them to the composition x = 0.4 by linear interpolation of the $\sin^2\theta_{ext}$ dependence within the x = 0.369 - 0.412 interval.

Table 2. Experimental and calculated phase-matching angles θ in $GaS_{0.4}Se_{0.6}$ for SHG and OPA processes in the mid-IR. Here λ denote(s) the input wavelength(s) and $\Delta\theta_{int} = \theta_{int}(exp) - \theta_{int}(calc)$ is the deviation of the internal angles.

process	λ [μm]	θ_{ext}(exp) [°]	θ_{ext}(calc) [°]	$\Delta\theta_{int}$ [']
SHG oo-e	2.79	43.76 [Ref. 8]	43.36	7
SHG oo-e	6.437	32.77 [Ref. 14]	33.42	13
SHG oo-e	9.58	48.42 [Ref. 8]	48.24	3
SHG oo-e	10.6	55.87 [Ref. 8]	55.46	6
OPA eo-e	1.0642(e) 1.275(o)	49.80 [Ref. 14]	49.38	6

The SHG (oo-e) phase-matching condition $n_o(\lambda) = n_e(\lambda/2, \theta_{int})$ together with $\sin\theta_{ext} = n_o(\lambda)\sin\theta_{int}$ leads to the following relation between $n_o(\lambda)$, $n_o(\lambda/2)$, $n_e(\lambda/2)$ and θ_{ext}: $\sin^2\theta_{ext} = [n_o^2(\lambda/2) - n_o^2(\lambda)]/[n_o^2(\lambda/2)/n_e^2(\lambda/2) - 1]$. In the chosen geometry for the OPA experiment,[14] the incident pump (e-wave) and signal (o-wave) beams were parallel. This leads to slightly noncollinear interaction inside the $GaS_{0.4}Se_{0.6}$ crystal but the angle between the signal (k_s) and pump (k_p) wave vectors does not exceed 0.1°. Taking into account that the cleaved crystal plates correspond to *c*-cut, the phase-matching condition, expressed as vanishing components of the phase-mismatch vector parallel and perpendicular to the *c*-axis, can be written as $P/\lambda_P - S/\lambda_S - I/\lambda_I = 0$, where $P^2 = n_o^2(\lambda_P)[1 - \sin^2\theta_{ext}/n_e^2(\lambda_P)]$, $S^2 = n_o^2(\lambda_S)[1 - \sin^2\theta_{ext}/n_o^2(\lambda_S)]$, $I^2 = n_o^2(\lambda_I)[1 - \sin^2\theta_{ext}/n_e^2(\lambda_I)]$, and λ_P, λ_S and λ_I, denote the pump, signal, and idler wavelengths, respectively.

The phase plate measurements were used to adjust the n_e values through the measured birefringence (Table 1) while the SHG and OPA experimental data was used to optimize the fit of both n_o and n_e. The resulting refined Sellmeier equations are summarized in Table 3.

Table 3. Refined Sellmeier equations for $GaS_{0.4}Se_{0.6}$, $n^2 = A_1 + A_3/(\lambda^2 - A_2) + A_5/(\lambda^2 - A_4)$, where λ is in μm, valid in the 0.63-10 μm spectral range.

crystal	n	A_1	A_2	A_3	A_4	A_5
$GaS_{0.4}Se_{0.6}$	n_o	9.830156	0.051856	0.306508	1467.12	4306.874
	n_e	7.295995	0.067716	0.251780	1197.31	2316.874

The new Sellmeier equations predict refractive indices at 1.0642 μm of $n_o = 2.67879$ and $n_e = 2.36549$, or a birefringence of ~0.31 at this wavelength. In Fig. 2, we compare the predictions of the new Sellmeier equations for type-I SHG with our initial approximation[10] and the predictions of the fits presented in Ref. 1 for this same composition. The same figure shows also all experimental results from Table 2 in the case of SHG. It is obvious that the old fits for the refractive indices from Ref. 1 are either erroneous or do not correspond to the specified composition of the crystal.

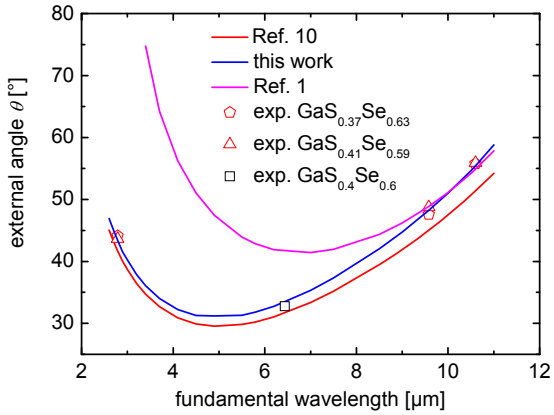

Fig. 2. SHG phase-matching in $GaS_{0.4}Se_{0.6}$ calculated using the new Sellmeier equations (blue line), our initial approximation (red line) from Ref. 10, and the old fits from Ref. 1 (violet line). The symbols correspond to the experimental SHG points from Ref. 8 and Ref. 14.

4. TWO-PHOTON ABSORPTION

Nonlinear absorption losses were studied with *c*-cut plates of 4.7 mm thickness ($GaS_{0.4}Se_{0.6}$) and 3.9 mm (GaSe) for o-polarization. A 10-Hz passive/active mode-locked Nd:YAG laser/amplifier (B. M. Industries) with M^2=1.3 was used at 1064 nm. The pulse duration (FWHM, assuming Gaussian pulses shape) measured by SHG autocorrelation, was 76 ps. The beam diameter inside the crystals was $2w$=0.24 mm. The measured nonlinear transmission for the two samples is shown in Fig. 3a as a function of the peak on-axis intensity calculated inside the crystals.

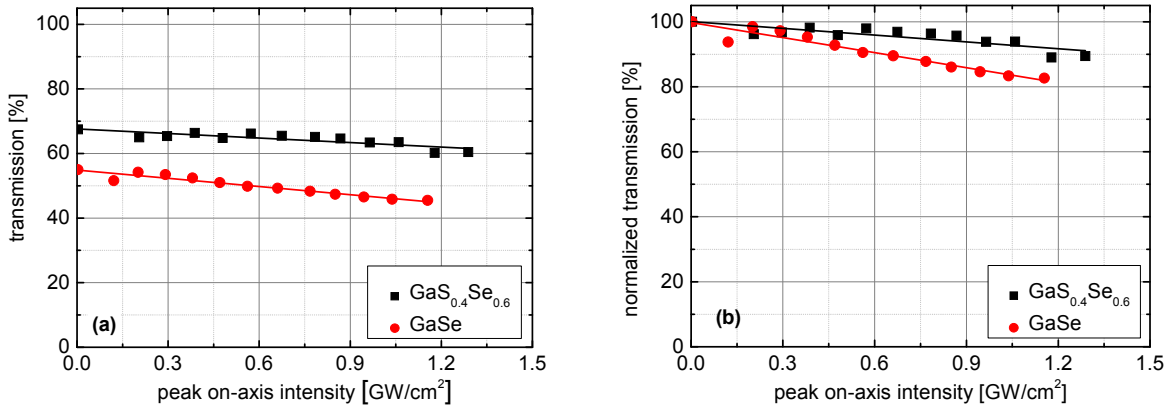

Fig. 3. (a) Measured nonlinear transmission of $GaS_{0.4}Se_{0.6}$ (black squares) and GaSe (red circles) in dependence on the peak on-axis intensity at 1064 nm calculated inside the crystal (taking into account the Fresnel reflection). The points at zero intensity are extrapolated from the given linear fits (lines) and agree very well with the low signal sample transmission taking into account the Fresnel reflections and the measured linear absorption coefficients. (b) The data from (a) corrected by the Fresnel reflections at normal incidence and the measured linear absorption.

The two crystals exhibit different linear absorption at this wavelength, which we estimated from independent measurements using a continuous-wave Nd:YVO_4 laser. The value of the linear absorption coefficient, 0.071 cm^{-1} for

$GaS_{0.4}Se_{0.6}$ and 0.29 cm^{-1} for GaSe were used then, together with the estimated Fresnel reflections, to arrive at the normalized nonlinear transmission shown in Fig. 3b.

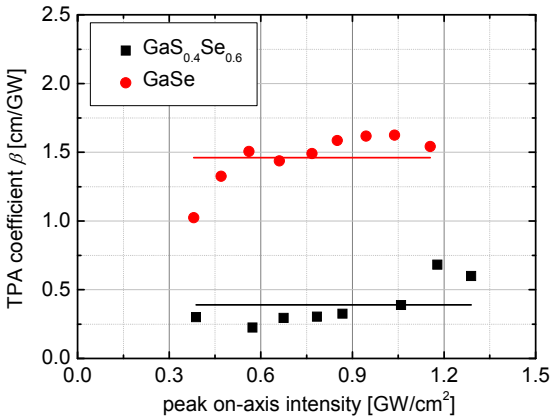

Fig. 4. TPA coefficient for $GaS_{0.4}Se_{0.6}$ (black squares) and GaSe (red circles) in dependence on the peak on-axis intensity at 1064 nm derived from the data presented in Fig. 3.

The TPA coefficient β was then calculated using well known expressions relating it to the normalized transmission, under the assumption of Gaussian temporal and spatial distribution and thin samples compared to the confocal parameter.[15] There is no dependence of the TPA coefficient on intensity in the intensity interval studied in Fig. 4 and the deviations from the constant fits were used to estimate the errors given. We obtained β=(0.415±0.07) cm/GW for $GaS_{0.4}Se_{0.6}$, and β =(1.46±0.13) cm/GW for GaSe.

For GaSe the result obtained is very close to the β=1.4 cm/GW, measured in Ref. 16 with 10 ps long pulses at a repetition rate of 81 MHz. The value obtained by us for $GaS_{0.4}Se_{0.6}$ is considerably smaller, which can be attributed to the larger band-gap.

Since GaSe and $GaS_{0.4}Se_{0.6}$ are negative uniaxial crystals, in a practical OPO scheme, the pump will be e-polarized. The TPA for the two polarizations was compared in Ref. 16 with the same GaSe sample by simply rotating it, and thus the ratio of 1.76 for the TPA coefficients can be considered to be very reliable. Assuming a similar ratio for $GaS_{0.4}Se_{0.6}$, one arrives at β~0.73 cm/GW for the e-polarization. Due to the large birefringence, phase matching angles are, however, small and for generation of idler wavelengths e.g. around 6.45 μm (θ~15° for oo-e interaction), the resulting value at the pump wavelength would be much closer to the experimental result for the o-wave. Peak on-axis intensities in the nanosecond (OPO) regime, in any crystal, usually do not exceed 50 MW/cm^2 in order to avoid surface damage. Thus the nonlinear losses in $GaS_{0.4}Se_{0.6}$ will be more than three times smaller than the linear losses for a crystal length of 1 cm which seems feasible for OPO having in mind the high effective nonlinearity.

It is clear that our TPA results in Fig. 4 are relevant not only to OPO operation but also to travelling-wave schemes like OPG and OPA which operate at higher intensities in the picosecond regime which require higher pump intensities.[17]

5. MICROHARDNESS

Indentation measurements with Berkovich indenter were carried out using a Nanoindenter XP (Agilent). This head possesses very high force and depth resolution and enables accurate measurements down to 100 μN maximum force or less. The Nanoindenter XP was equipped with a so-called continuous stiffness monitor (CSM). This makes it possible to measure the complete modulus and hardness depth dependence performing only one test cycle. The Berkovich indenter was of the so-called AccuTip type (MTS Systems Corporation). These are very sharp tips with a nominal tip radius of about 50 nm.

Measurements with maximum indentation depth of 500 nm were carried out on $GaS_{0.4}Se_{0.6}$ and GaSe samples. Each of them was repeated 10 times. The force increase to the maximum value was applied at a constant strain rate of 0.051/s. For the CSM, an additional harmonic oscillation with amplitude of 2 nm and frequency of 45 Hz was used. From the measured harmonic contact stiffness, the Young's modulus was determined according to the Oliver and Pharr method.[18]

A set of typical load versus displacement curves for maximum loads of 4.5 mN taken for GaSe is shown in Fig. 5a. Pop-in processes are easily observed in the course of plastic deformation. In Fig. 5b, the initial parts of the load versus displacement curves, up to a load of 0.5 mN, are shown. It is clear that pop-in processes become significant only with at indentation depths greater than 60 nm. Figure 6a shows that the modulus value calculated from the CSM data is constant with indentation depth up to an indentation depth of 100 nm. For the average value at 50 nm indentation depth it was found that E_{IT} = (33.2 ± 1.2) GPa (assuming a Poisson ratio of 3.5). The constant behavior of the hardness with increasing indentation depth calculated from the CSM data up to an indentation depth of 60 nm is shown in Fig. 6b. For the average value at 50 nm indentation depth it was found that H_{IT} = (2.55 ± 0.06) GPa. The modulus values found for GaSe are in very good agreement with the data published in Ref. 19: E_{IT} = (33 ± 3) GPa.

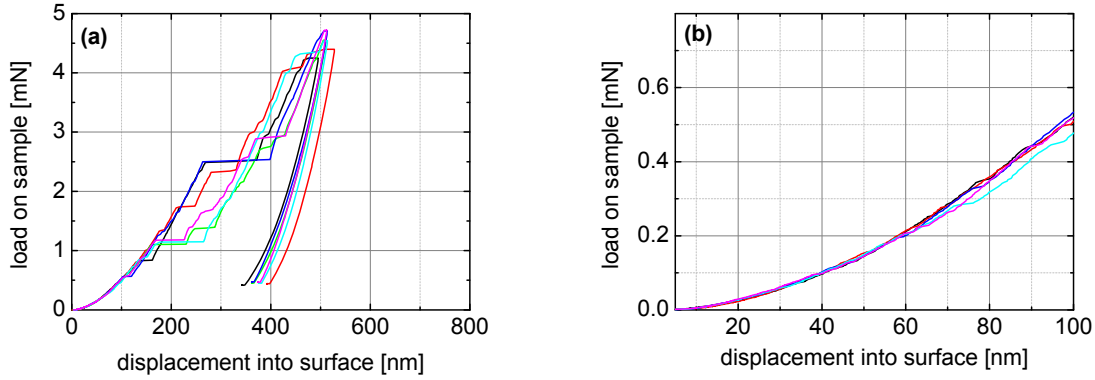

Fig. 5. Load versus displacement curves for GaSe.

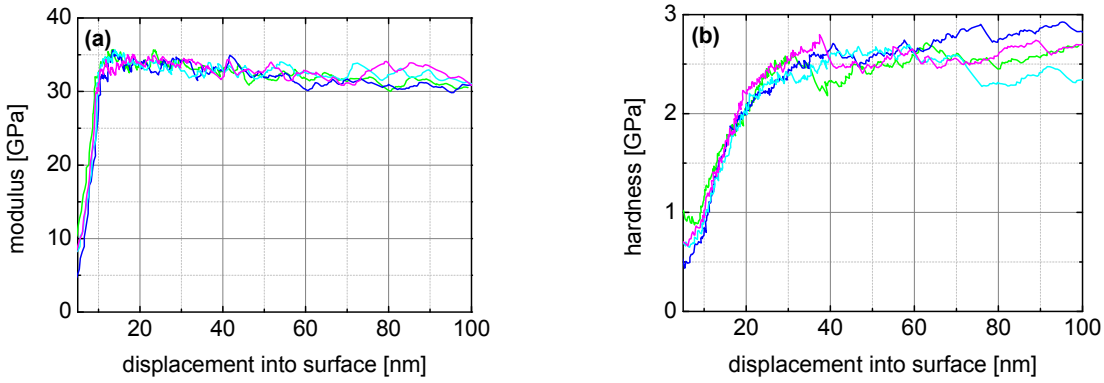

Fig. 6. Modulus and hardness of GaSe versus displacement.

A set of typical load versus displacement curves for maximum loads of 6.5 mN taken for $GaS_{0.4}Se_{0.6}$ is shown in Fig. 7a. Pop-in processes are easily observed in the course of plastic deformation. In Fig. 7b, the first parts of the load versus displacement curves, up to a load of 0.5 mN, are shown. It is clear that pop-in processes become significant already at indentation depths greater than 30 nm. Figure 8a shows that the modulus value calculated from the CSM data is not constant with indentation depth. For the average value at 50 nm indentation depth it was found that E_{IT} = (36.8 ± 4.5) GPa (assuming a Poisson ratio of 3.5). At an indentation depth of 10 nm it was found that E_{IT} = (39.4 ± 2.8) GPa. The hardness is also not constant with increasing indentation depth as can be seen from Fig. 8b. For the average value at

50 nm indentation depth it was found that H_{IT} = (3.27 ± 0.33) GPa and for 20 nm indentation depth H_{IT} = (3.45 ± 0.43) GPa.

In comparison with GaSe the values found for the indentation modulus and the indentation hardness of $GaS_{0.4}Se_{0.6}$ are about 30% higher. A formal correlation between H_{IT} (MPa) and HV (kgf/mm²) exists and H_{IT} = 1 GPa can be correlated to 94.5 HV. The higher microhardness of $GaS_{0.4}Se_{0.6}$ will make it easier for cutting and polishing.

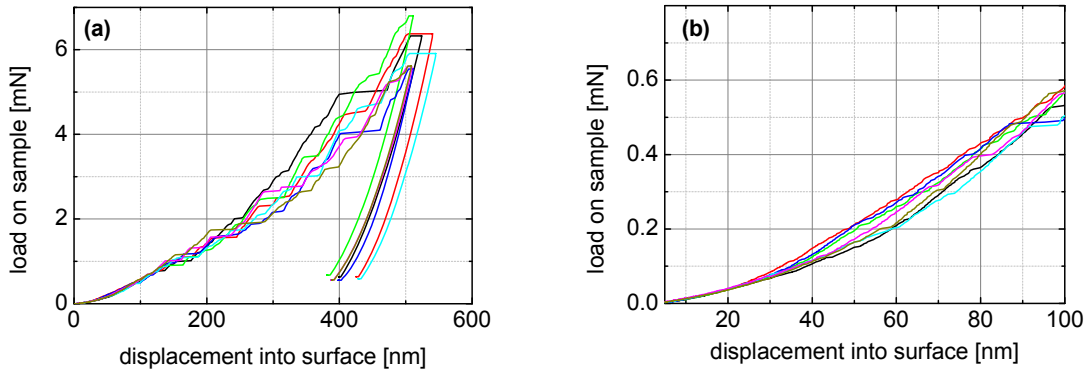

Fig. 7. Load versus displacement curves for $GaS_{0.4}Se_{0.6}$.

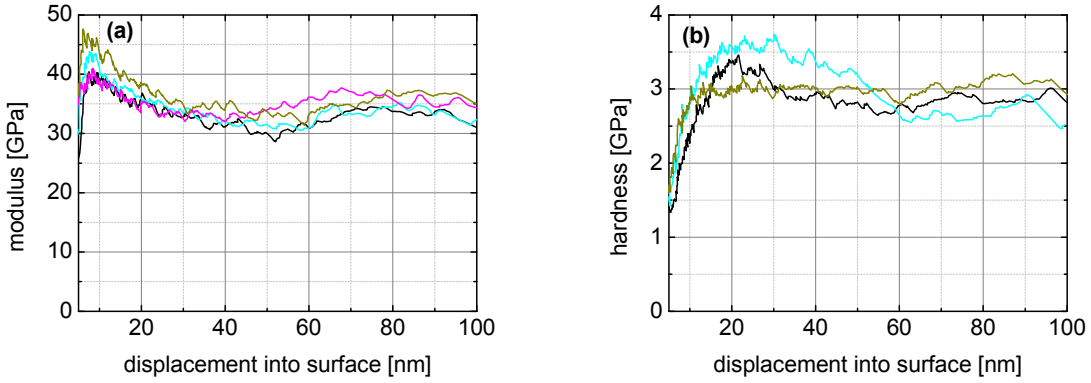

Fig. 8. Modulus and hardness of $GaS_{0.4}Se_{0.6}$ versus displacement.

6. CONCLUSION

$GaS_{0.4}Se_{0.6}$ exhibits larger band-gap value in comparison to GaSe while its nonlinear coefficient d_{22} is reduced by only 24%. The increased band-gap leads to higher surface damage threshold and enables pumping at shorter laser wavelengths. Our preliminary Sellmeier equations for $GaS_{0.4}Se_{0.6}$ were based on refractive index measurements. These equations were refined in the present work by fitting second-harmonic generation and optical parametric amplification phase-matching angle data in the mid-infrared as well as birefringence data in the visible and near-infrared obtained with thin phase retardation plates. The two-photon absorption effect was compared for $GaS_{0.4}Se_{0.6}$ and GaSe using amplified picosecond pulses at 1064 nm, at intensities in the GW/cm^2 range. The two-photon absorption coefficient of $GaS_{0.4}Se_{0.6}$ for the o-polarization is 3.5 times smaller than the corresponding coefficient of GaSe. Thus $GaS_{0.4}Se_{0.6}$ seems promising for use in Nd:YAG laser pumped nanosecond optical parametric oscillators or picosecond optical parametric amplifiers, without nonlinear absorption losses. The dynamic indentation measurements with Berkovich type indenter of *c*-cut

$GaS_{0.4}Se_{0.6}$ and GaSe plates indicate about 30% higher indentation modulus and microhardness of $GaS_{0.4}Se_{0.6}$ in comparison to GaSe.

ACKNOWLEDGMENTS

The research leading to these results has received funding from the European Community's Seventh Framework Programme FP7/2007-2011 under grant agreement n°224042.

REFERENCES

1. K. R. Allakhverdiev, R. I. Guliev, É. Yu. Salaev, and V. V. Smirnov, "Investigation of linear and nonlinear optical properties of GaS_xSe_{1-x} crystals," Sov. J. Quantum Electron. **12**, 947-948 (1982) [transl. from Kvantovaya Elektron. (Moscow) **9**, 1483-1485 (1982)].
2. H. Serizawa, Y. Sasaki, and Y. Nishina, "Polytypes and excitons in $GaSe_{1-x}S_x$ mixed crystals," J. Phys. Soc. Japan **48**, 490-495 (1980).
3. C. H. Ho, C. C. Wu, and Z. H. Cheng, "Crystal structure and electronic structure of $GaSe_{1-x}S_x$ series layered solids," J. Cryst. Growth **279**, 321-328 (2005).
4. K. R. Allakhverdiev, M. Ö. Yetis, S. Özbek, T. K. Baykara, and E. Yu. Salaev, "Effective nonlinear GaSe crystal. Optical properties and applications," Las. Phys. **19**, 1092-1104 (2009).
5. G. B. Abdullaev, K. R. Allakhverdiev, R. Kh. Nani, E. Yu. Salaev, and M. M. Tagyev, "Neutron diffraction, infrared, and Raman scattering investigations of the layered GaS_xSe_{1-x} system," phys. stat. sol. (a) **53**, 549-555 (1979).
6. C. Perez Leon, L. Kador, K. R. Allakhverdiev, T. Baykara, and A. A. Kaya, "Comparison of the layered semiconductors GaSe, GaS, and $GaSe_{1-x}S_x$ by Raman and photoluminescence spectroscopy," J. Appl. Phys. **98**, 103103 (2005).
7. S. Das, C. Ghosh, O. G. Voevodina, Yu. M. Andreev, and S. Yu. Sarkisov, "Modified GaSe crystal as a parametric frequency converter," Appl. Phys. B **82**, 43-46 (2006).
8. H.-Z. Zhang, Z.-H. Kang, Y. Jiang, J.-Y. Gao, F.-G. Wu, Z.-S. Feng, Y. M. Andreev, G. V. Lanskii, A. N. Morozov, E. I. Sachkova, and S. Yu. Sarkisov, "SHG phase matching in GaSe and mixed $GaSe_{1-x}S_x$, $x \leq 0.412$, crystals at room temperature," Opt. Exp. **16**, 9951-9957 (2008).
9. A. Gouskov, J. Camassel, and L. Gouskov, "Growth and characterization of III-VI layered crystals like GaSe, GaTe, InSe, $GaSe_{1-x}Te_x$ and $Ga_xIn_{1-x}Se$," Prog. Crystal Growth and Charact. **5**, 323-413 (1982).
10. V. Petrov, V. L. Panyutin, A. Tyazhev, G. Marchev, A. I. Zagumennyi, F. Rotermund, F. Noack, K. Miyata, L. D. Iskhakova, and A. F. Zerrouk, "$GaS_{0.4}Se_{0.6}$: relevant properties and potential for 1064 nm pumped mid-IR OPOs and OPGs operating above 5 μm," Las. Phys. **21**, (2011), in press.
11. G. A. Akhundov, N. A. Gasanova, and M. A. Nizametdinova, "Optical absorption, reflection, and dispersion of GaS and GaSe layer crystals," phys. stat. sol. (b) **15**, K109-K113 (1966).
12. C. C. Wu, C. H. Ho, W. T. Shen, Z. H. Cheng, Y. S. Huang, and K. K. Tiong, „Optical properties of $GaSe_{1-x}S_x$ series layered semiconductors grown by vertical Bridgman method," Mater. Chem. Phys. **88**, 313-317 (2004).
13. P. G. Rustamov, Z. D. Melnikova, M. G. Safarov, and M. A. Alidzhanov, "Solid solutions in the system GaS – GaSe," Inorg. Mat. **1**, 387-389 (1965) [transl. from Izv. Akad. Nauk. SSSR, Neorganicheskie Materialy, **1**, 419-421 (1965)].
14. K. Miyata, G. Marchev, A. Tyazhev, V. Panyutin, and V. Petrov, "Picosecond mid-IR optical parametric amplifier based on $GaS_{0.4}Se_{0.6}$ pumped by a Nd:YAG laser system at 1064 nm," Conference on Lasers and Electro-Optics, CLEO'2011, submitted.

15. R. L. Sutherland, *Handbook of Nonlinear Optics*, Second Edition, Marcel Dekker, 2003.

16. K. R. Allakhverdiev, T. Baykara, S. Joosten, E. Günay, A. A. Kaya, A. Kulibekov (Gulubayov), A. Seilmeier, and E. Yu. Salaev, "Anisotropy of two-photon absorption in gallium selenide at 1064 nm," Opt. Commun. **261**, 60-64 (2006).

17. T. Dahinten, U. Plödereder, A. Seilmeier, K. L. Vodopyanov, K. R. Allakhverdiev, and Z. A. Ibragimov, „Infrared pulses of 1 picosecond duration tunable between 4 μm and 18 μm," IEEE J. Quantum Electron. **29**, 2245-2250 (1993).

18. W.C. Oliver and G.M. Pharr, "An improved technique for determining hardness and elastic modulus using load and displacement sensing indentation experiments," J. Mater. Res. **7**, 1564-1583 (1992).

19. D. H. Mosca, N. Mattoso, C. M. Lepienski, W. Veiga, I. Mazzaro, V. H. Etgens, and M. Eddrief, "Mechanical properties of layered InSe and GaSe single crystals," J. Appl. Phys. **91**, 140 -144 (2002).